3D Finite Element Analysis of Nutrient Distributions and Cell Viability in the Intervertebral Disc: Effects of Deformation and Degeneration

Alicia R. Jackson
Tissue Biomechanics Lab,
Department of Biomedical Engineering,
University of Miami,
Coral Gables, FL 33146;
Department of Orthopaedics,
University of Miami Miller School of Medicine,
Miami, FL 33136

Chun-Yuh C. Huang
Stem Cell and Mechanobiology Lab,
Department of Biomedical Engineering,
University of Miami,
Coral Gables, FL 33146

Mark D. Brown
Department of Orthopaedics,
University of Miami Miller School of Medicine,
Miami, FL 33136

Wei Yong Gu[1]
Tissue Biomechanics Lab,
Department of Biomedical Engineering,
University of Miami,
Coral Gables, FL 33146;
Department of Mechanical and
Aerospace Engineering,
University of Miami,
Coral Gables, FL 33146
e-mail: wgu@miami.edu

The intervertebral disc (IVD) receives important nutrients, such as glucose, from surrounding blood vessels. Poor nutritional supply is believed to play a key role in disc degeneration. Several investigators have presented finite element models of the IVD to investigate disc nutrition; however, none has predicted nutrient levels and cell viability in the disc with a realistic 3D geometry and tissue properties coupled to mechanical deformation. Understanding how degeneration and loading affect nutrition and cell viability is necessary for elucidating the mechanisms of disc degeneration and low back pain. The objective of this study was to analyze the effects of disc degeneration and static deformation on glucose distributions and cell viability in the IVD using finite element analysis. A realistic 3D finite element model of the IVD was developed based on mechano-electrochemical mixture theory. In the model, the cellular metabolic activities and viability were related to nutrient concentrations, and transport properties of nutrients were dependent on tissue deformation. The effects of disc degeneration and mechanical compression on glucose concentrations and cell density distributions in the IVD were investigated. To examine effects of disc degeneration, tissue properties were altered to reflect those of degenerated tissue, including reduced water content, fixed charge density, height, and endplate permeability. Two mechanical loading conditions were also investigated: a reference (undeformed) case and a 10% static deformation case. In general, nutrient levels decreased moving away from the nutritional supply at the disc periphery. Minimum glucose levels were at the interface between the nucleus and annulus regions of the disc. Deformation caused a 6.2% decrease in the minimum glucose concentration in the normal IVD, while degeneration resulted in an 80% decrease. Although cell density was not affected in the undeformed normal disc, there was a decrease in cell viability in the degenerated case, in which averaged cell density fell 11% compared with the normal case. This effect was further exacerbated by deformation of the degenerated IVD. Both deformation and disc degeneration altered the glucose distribution in the IVD. For the degenerated case, glucose levels fell below levels necessary for maintaining cell viability, and cell density decreased. This study provides important insight into nutrition-related mechanisms of disc degeneration. Moreover, our model may serve as a powerful tool in the development of new treatments for low back pain. [DOI: 10.1115/1.4004944]

Keywords: glucose, annulus fibrosus, nucleus pulposus, mechanical loading, cell density

Introduction

Each year, millions of Americans experience symptoms of low back pain, resulting in annual expenditures exceeding $50 billion, in both direct and indirect costs [1,2]. While the exact cause of low back pain remains unclear, degeneration of the intervertebral discs (IVD) of the spine has been implicated as a possible source leading to the condition [3–6]. Several factors may lead to the onset of disc degeneration, including lack of proper nutritional supply, abnormal mechanical loading, and genetic factors [7].

The intervertebral disc is composed of three regions, which have distinct compositions and functions: nucleus pulposus (NP), annulus fibrosus (AF), and cartilaginous endplate (CEP), see Fig. 1(*a*). The NP is located at the center of the disc and is composed of randomly oriented collagen fibers in a proteoglycan gel. The AF surrounds the NP and consists of 15–25 concentric lamellae made up of highly organized collagen fiber bundles [8,9]. The CEP is located at the interface between the vertebrae and the NP and inner one-third of the AF; it has a make-up similar to that of hyaline cartilage.

Although sparse [10], the cells of the IVD play an important role in maintaining the disc extracellular matrix, which is vital to preserving the biomechanical function of the IVD in the spine. To this end, disc cells must produce both matrix proteins and catabolic molecules necessary for matrix breakdown [11]; an imbalance in these results in the onset of disc degenerative changes [12,13]. In order to perform this function properly, disc cells require nutrients, including glucose and oxygen, to provide the necessary energy for cellular activity.

Because the disc is avascular, essential nutrients must be transported by diffusion through the tissue from the surrounding

[1]Corresponding author.

Contributed by the Bioengineering Division of ASME for publication in the JOURNAL OF BIOMECHANICAL ENGINEERING. Manuscript received July 12, 2011; final manuscript received August 22, 2011; published online October 11, 2011. Editor: Michael Sacks.

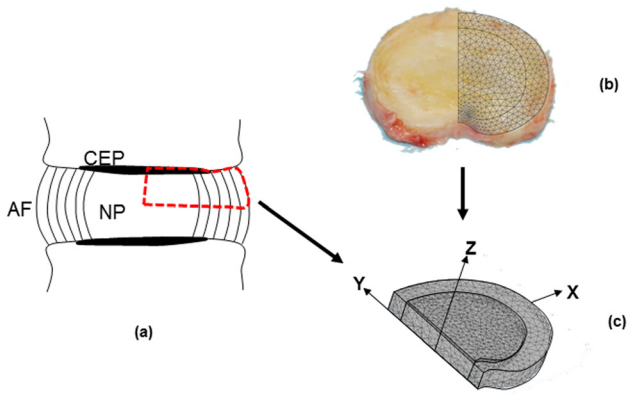

Fig. 1 (*a*) Schematic of the intervertebral disc showing the annulus fibrosus (AF), nucleus pulposus (NP), and cartilaginous endplate (CEP) regions; (*b*) photograph of human L2-L3 disc using for determining disc geometry; (*c*) mesh of upper right quarter of disc.

vasculature, either at the periphery of the AF (i.e., periannular route) or from the vasculature located in the vertebral body adjacent to the CEP (i.e., endplate route) [14–24]. Since nutrients must be transported in, concentration gradients can develop across the disc and are dependent upon the supply of nutrients, the rate of nutrient transport through the IVD extracellular matrix, and the rate of cellular metabolism by disc cells. A change in any of these factors will alter the balance in the disc and may have detrimental effects on the tissue and cells since local concentrations of nutrients and metabolites have been shown to have a significant effect on cellular activity and survival [7,15,25–31]. For instance, a fall in nutrient supply at the disc periphery, caused by an obstruction of the supply above the cartilaginous endplate in the case of calcification or other degenerative changes to the IVD, may significantly affect the nutritional supply to the disc. Likewise, mechanical loading, particularly, sustained compression, may reduce nutrient transport rates through the tissue.

Glucose has been identified as the critical nutrient necessary for IVD cell survival [15,25,32,33]. It has generally been found that IVD cells rely primarily on glycolysis (i.e., the breakdown of glucose to lactic acid) for energy metabolism [20,26]. Furthermore, previous *in vitro* studies have shown that IVD cells require minimum levels of glucose (i.e., 0.5 mM) to maintain viability [15,25,32,34] while they can survive for long periods in the absence of oxygen [15]. Therefore, knowledge of glucose distributions in the disc under various conditions, such as mechanical loading and degeneration, is crucial to understanding nutrition-related mechanisms of cell death and subsequent disc degenerative changes.

The study of *in vivo* cellular activity and nutrient distributions in the IVD is difficult, particularly in human discs. Finite element modeling (FEM) of the disc can therefore serve as an important supplement to experimental results in order to fully understand the *in vivo* environment in the IVD. Several previous investigators have presented FE models of the intervertebral disc in order to examine nutrient supply and distributions in the tissue [33,35–41]. Most recently, Shirazi-Adl et al. analyzed the cell viability in the IVD using a finite element model [33]. However, this model did not consider a realistic, 3D geometry, but rather a two-dimensional axisymmetric geometry of the disc, nor did it include tissue properties that were coupled to deformation of the tissue. These features are critical in the development of an accurate numerical model of the IVD, which may provide necessary information in order to develop new strategies for treating and/or curbing the effect of disc degeneration and related low back pain.

In this study, we extend our previous finite element formulation of the intervertebral disc [41], which includes a three-dimensional anatomical disc geometry, tissue properties coupled to mechanical deformation, and nutrient concentrations coupled to cellular metabolism, to include cell viability criteria based on threshold levels of glucose necessary for cellular survival. Using this model, we can predict effects of nutrient concentration on the density distribution of cells in the IVD. We hypothesized that degenerative changes and static deformation will alter glucose distributions in the IVD and may also cause a loss of cell viability resulting from poor nutritional supply to disc cells. To test these hypotheses, we have investigated the effects of disc degeneration, including reduced endplate permeability (as is the case for endplate calcification), and mechanical deformation (i.e., 10% static compressive strain) on the glucose distributions and cell viability in the IVD.

Method of Approach

Theoretical Formulation. The theoretical framework of our model was based on the mechano-electrochemical mixture theory [42]. The governing equations are based on the balance of linear momentum and conservation of mass

$$\nabla \cdot \boldsymbol{\sigma} = 0 \tag{1}$$

$$\nabla \cdot (v^s + J^w) = 0 \tag{2}$$

$$\frac{\partial(\phi^w c^\alpha)}{\partial t} + \nabla \cdot (J^\alpha + \phi^w c^\alpha v^s) = Q^\alpha \tag{3}$$

where $\boldsymbol{\sigma}$ is the total stress of the mixture, v^s is the velocity of the solid phase, J^w and J^α are the molar fluxes of the water and solute α phases, respectively, relative to the solid phase, ϕ^w is the tissue porosity (water volume fraction), c^α is the concentration (per unit water volume) of solute α, and Q^α is the cellular metabolic rate of solute α per unit tissue volume. The total stress on the mixture can be expressed as

$$\sigma = -p\mathbf{I} + \lambda tr(\mathbf{E})\mathbf{I} + 2\mu\mathbf{E} \tag{4}$$

where p is the fluid pressure, $\mathbf{I}$ is the identity tensor, λ and μ are the elastic (Lamé) coefficients of the solid matrix, $\mathbf{E}$ is the infinitesimal strain tensor for the solid matrix, and $tr(\mathbf{E})$ is the dilatation (e). Additionally, the fluid flux, J^w, and the solute flux, J^α, can be expressed in terms of the water chemical potential, μ^w, and the solute (electro)chemical potential, $\tilde{\mu}^\alpha$

$$J^w = -k\left(\rho_T^w \nabla\mu^w + \sum_\alpha H^\alpha c^\alpha M^\alpha \nabla\tilde{\mu}^\alpha\right) \tag{5}$$

$$J^\alpha = H^\alpha c^\alpha J^w - \frac{D^\alpha \rho^\alpha}{RT}\nabla\tilde{\mu}^\alpha \tag{6}$$

where k is the hydraulic permeability, ρ_T^w is the true mass density of water, H^α is the convection coefficient (also known as the hindrance factor) of solute α, $M^\alpha$is the molar weight of solute α, D^α is the diffusivity of solute α, ρ^α is the apparent mass density, and R and T are universal gas constant and absolute temperature, respectively.

The IVD was modeled as a mixture of solid (matrix) phase, fluid (water) phase, and solute phase; solutes considered were ions (Na^+ and Cl^-), glucose, oxygen, and lactate. Deformation-dependent tissue properties, including tissue porosity, fixed charge density, hydraulic permeability, and solute diffusivities [42–44], have been incorporated into the model in order to most accurately reflect the *in vivo* environment in the disc under compression. The porosity (or water volume fraction) of the tissue in the compressed state, ϕ^w, is related to the tissue dilatation, e, and the porosity of the undeformed tissue, ϕ_o^w

$$\phi^w = \frac{\phi_o^w + e}{1 + e} \tag{7}$$

The hydraulic permeability of the tissue, k, was determined from the following constitutive relation [43]

$$k = a\left(\frac{\phi^w}{1-\phi^w}\right)^n \tag{8}$$

where a and n are parameters whose values depend on the composition and structure of the tissue and therefore vary by region in the disc. The diffusivity of solute α, D^α, was estimated based on the constitutive relationship [44]

$$\frac{D^\alpha}{D_o^\alpha} = \exp\left[-A\left(\frac{r^\alpha}{\sqrt{k}}\right)^B\right] \tag{9}$$

where D_o^α is the diffusivity of solute α in aqueous solution, r^α is the hydrodynamic radius of solute α, and A and B are material constants previously determined for agarose gel and IVD tissues. Since both permeability and diffusivity are dependent upon tissue porosity and porosity varies with the tissue dilatation according to Eq. (7), these parameters are also strain-dependent. In our model, the Na^+ (c^+) and Cl^- (c^-) concentrations are related through the electroneutrality condition, $c^+ = c^- + c^F$, where c^F is the fixed charge density of the tissue, which depends on tissue porosity by

$$c^F = \frac{c_o^F(1-\phi^w)\phi_o^w}{(1-\phi_o^w)\phi^w} \tag{10}$$

where c_o^F is the fixed charge density in reference configuration. Hence, in this model formulation, the tissue properties are coupled to mechanical deformation of the tissue.

Cell Viability Criteria. We have included criteria for maintaining cell viability in our model using threshold levels of nutrients necessary for cell survival. Previous studies have shown that glucose is the critical nutrient needed by IVD cells: disc cells begin to die when glucose levels fall below 0.5 mM [15,25,32,34]. In our model, the cell density varies with the glucose concentration, decreasing (i.e., cells begin to die) when the glucose concentration falls below 0.5 mM and continuing in a linear fashion until levels fall to 0.2 mM, at which point the cell density reaches zero (i.e., all cells die), see Fig. 2.

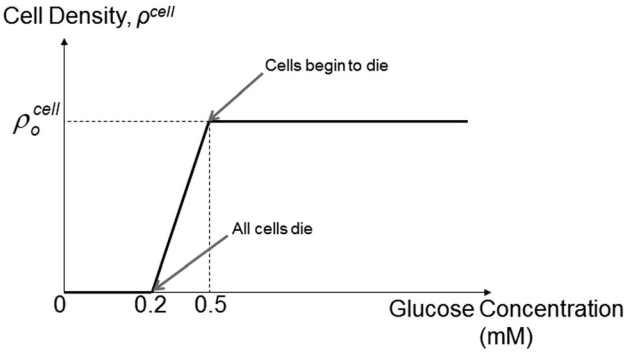

Fig. 2 Criteria for cell viability based on threshold levels of glucose. Cell density varies with glucose concentration: when glucose levels fall below 0.5 mM, cell density decreases (i.e., cells begin to die) in a linear fashion until reaching 0.2 mM, when cell density reaches zero (i.e., all cells die).

Finite Element Model. As in our prior study [41], we considered a realistic, three-dimensional (3D) anatomical disc geometry based on that of an L2-L3 human disc (see Fig. 1(*b*)). The IVD was harvested from the spine of a 41-year old male during autopsy and was graded as a normal, grade I disc according to the Thompson morphological grading scheme [45]. The disc dimensions were determined using a photograph of the harvested disc and ImageJ software (National Institutes of Health, Bethesda, MD). The disc was considered an inhomogeneous material consisting of three distinct regions: AF, NP, and CEP. Because of symmetry, only the upper right quarter of the IVD was modeled (Fig. 1(*c*)). The mesh consisted of approximately 6900 second order, tetrahedral Lagrange elements. Mesh convergence was determined based on the solute concentrations. The FEM formulation, employing the weak form, was based on the work by Sun et al. [46] and has been extended from our previous works [35,41,47]. COMSOL software (Comsol 3.2, COMSOL, Inc., Burlington, MA) was used to solve the three-dimensional boundary value problem.

Tissue Properties and Cellular Activity. Properties used in the model were based on experimental results in the literature [16,44,47–55] and are shown in Table 1. All values of convection

Table 1 IVD tissue properties incorporated into the model

		AF	NP	CEP
Reference water content, ϕ_o^w	*Normal:*	0.75 [48]	0.86 [48]	0.60 [49,50]
	Degenerated:	0.68	0.78	0.30
ρ^{cell} (cells/mm^3) [16]		9000	4000	15000
c^F (mol/m^3)	*Normal:*	150	250	90
	Degenerated:	125	175	90
Parameters for diffusivity[a]	$\frac{D^\alpha}{D_o^\alpha} = \exp\left[-A\left(\frac{r^\alpha}{\sqrt{k}}\right)^B\right]$	$A = 1.29$ $B = 0.372$	$A = 1.25$ $B = 0.681$	$A = 1.29$ $B = 0.372$
Parameters for permeability	$k = a\left(\frac{\phi^w}{1-\phi^w}\right)^n$	$a = 0.00044$ nm^2 [b] $n = 7.193$[b]	$a = 0.00339$ nm^2 [c] $n = 3.24$[c]	$a = 0.0248$ nm^2 [d] $n = 2.154$[d]
Elasticity (Lamé) constants	*Normal:*	$\lambda = 0.30$ MPa [53] $\mu = 0.10$ MPa [53]	$\lambda = 15.6$ kPa[e] $\mu = 0.18$ kPa[e]	$\lambda = 0.10$ MPa [47] $\mu = 0.20$ MPa [47]
	Degenerated:	$\lambda = 0.70$ MPa [53] $\mu = 0.15$ MPa [53]	$\lambda = 25.8$ kPa[e] $\mu = 0.61$ kPa[e]	$\lambda = 0.10$ MPa [47] $\mu = 0.20$ MPa [47]

[a]Values for porcine AF tissue (AF and CEP) and agarose gels (NP) [44].
[b]Values for porcine AF tissue (AF) [51].
[c]Values for agarose gels (NP) [43].
[d]From Yao and Gu [47], curve-fit from Fig. 9 of Maroudas [52].
[e]Calculated from results in Iatridis et al., [54] and Johannessen and Elliot [55].

Table 2 Specific boundary conditions

	Solid matrix	Solute flux
Plane $x=0$	$u_x = \sigma_{xy} = \sigma_{xz} = 0$	$J^\alpha = 0$
Plane $z=0$	$u_z = \sigma_{zx} = \sigma_{zy} = 0$	$J^\alpha = 0$
Top surfaces	$u_z = \begin{cases} 0 & \text{reference} \\ -0.1 * h & \text{deformed} \end{cases}$	AF: $J^\alpha = 0$ CEP: $\tilde{\mu}^\alpha = \tilde{\mu}^{\alpha *}$ Solute concentration in surrounding media: $c^{glu} = 4$ mM; $c^{O_2} = 5.1$ kPa; $c^{lac} = 0.8$ mM; $c^+ = c^- = 0.15$ M
Lateral AF surface	$\sigma \cdot \vec{n} = 0$	$\tilde{\mu}^\alpha = \tilde{\mu}^{\alpha *}$ Solute concentration in surrounding media: $c^{glu} = 5$ mM; $c^{O_2} = 5.8$ kPa; $c^{lac} = 0.9$ mM; $c^+ = c^- = 0.15$ M

u is the solid displacement.
α = glucose (glu), oxygen (O_2), lactate (lac), Na^+ ion (+), Cl^- ion (−).
$\tilde{\mu}^\alpha = \tilde{\mu}^{\alpha *}$ signifies that (electro)chemical potential is continuous at the tissue boundary (* denotes quantity in external solution).

coefficients for ions and nutrients were assumed to be unity because of the size of molecules. For normal IVD, the AF and NP regions had a uniform thickness of 10 mm; the CEP had a thickness of 0.6 mm and was considered as permeable above the NP region only. Degenerated IVD tissue is known to have lower water content and fixed charge density, as well as reduced disc height, as compared with nondegenerated (i.e., normal) tissue. Furthermore, the disc becomes stiffer with degeneration, altering the values of elastic (Lamé) constants for the tissue. The properties used for modeling degenerated disc are also shown in Table 1. Additionally, the heights of the AF and NP regions of the disc were reduced by 10% to $h = 9$ mm.

During degeneration, the cartilage endplate is known to become calcified, thereby hindering the transport of solutes between the disc and the vasculature in the subchondral bone adjacent to the endplate [14,56–59]. In order to simulate calcification, the permeability of the tissue was reduced by decreasing the water content of the CEP tissue by 50% to 0.30 (see Table 1). This reduction resulted in a 93% decrease in the hydraulic permeability of the tissue, based on the previously developed constitutive equation for hydraulic permeability in charged, hydrated soft tissues, shown in Eq. (8).

Rates of cellular metabolism incorporated were the same as those used in our previous study [41] and were based on experimental results in the literature for IVD cells [60,61]. The rates of metabolism of Na^+ and Cl^- ions were considered to be zero. Due to a lack of experimental results in the literature, metabolic rates did not differ for normal and degenerated IVD cells. Metabolic rates for chondrocytes in the cartilage endplate region were considered the same as those for annulus fibrosus cells.

Boundary Conditions. The specific boundary conditions taken into consideration in this study are shown in Table 2. Initial solute concentrations in the surrounding media were the same as those used in our previous models [35,41]. Note that the axial AF edge is considered as impermeable. In this study, we have investigated how mechanical deformation affects glucose concentrations and related cell viability in normal and degenerated IVD using our model. A 10% static compressive strain was applied to the tissue using a displacement boundary condition (see configuration in Fig. 3). The final results are for the disc at equilibrium following the application of strain to the IVD (where applicable) and therefore represent the effects of long-term compressive loading (or deformation) on the IVD.

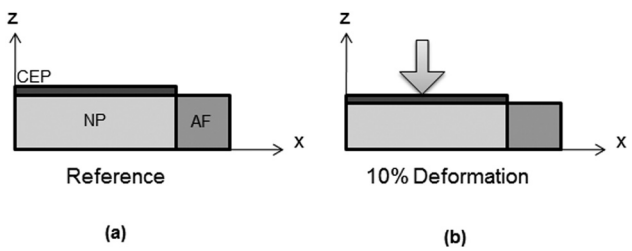

Fig. 3 Schematic showing (*a*) reference configuration, without deformation; (*b*) deformation configuration, with 10% static axial compression

Results

The results of this study indicate that degeneration and static compression both affect the glucose levels and related cell viability in the IVD. Results for glucose distribution in normal and degenerated IVD are shown in Fig. 4. For all cases, the minimum glucose concentrations in the disc were located at the lateral interface between the AF and NP regions, at the center (or mid-plane) of the disc.

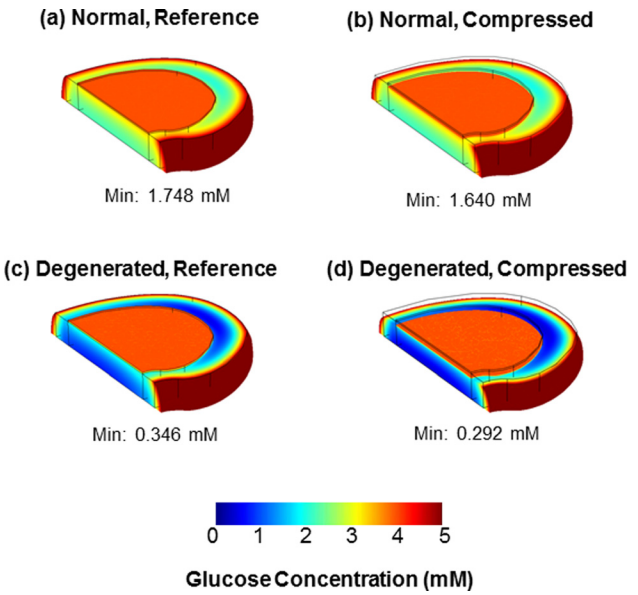

Fig. 4 Glucose distributions and minimum concentrations in the IVD for the four cases investigated: (*a*) normal disc in reference (i.e., undeformed) configuration; (*b*) normal disc in deformed configuration; (*c*) degenerated disc in reference configuration; (*d*) degenerated disc in deformed configuration

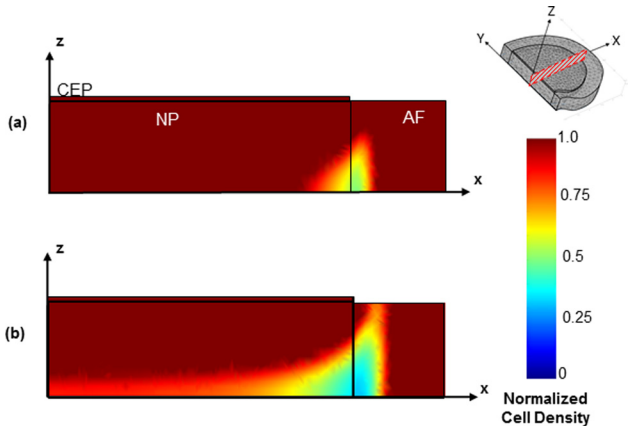

Fig. 5 Normalized cell density in the degenerated disc for (*a*) reference and (*b*) deformed cases. Note that the density is for the slice shown in the upper left is shown. Cell density values are normalized by original values (see Table 1).

Our results show that degenerative changes to the disc result in an 80% decrease in the minimum glucose concentration in the IVD. This effect was predominant in the NP region of the disc, in which there was 60% decrease in the averaged glucose concentration, as compared with a 40% decrease in the AF region. The glucose concentration distributions in normal and degenerated IVD in the reference configuration (i.e., no deformation) are shown in Figs. 4(*a*) and 4(*c*); note that, for the degenerated case, the majority of the disc volume is represented in dark blue, signifying that very low glucose concentrations are present in most of the tissue.

In this study, we have shown that changing tissue properties to reflect degenerated tissue allows us to predict changes in cell viability with disc degeneration. The averaged cell density fell 11% in the disc as a result of degenerative changes to the tissue, compared to results for the normal disc in reference configuration. The change in cell density for the degenerated disc in reference configuration can be seen in Fig. 5(*a*). As expected, no change in cell density distributions was found to occur in the normal tissue (data not shown).

Mechanical deformation affected both the nutrient and cell density distributions in the IVD; results are shown in Figs. 4(*b*), 4(*d*), and 5(*b*). For normal IVD, the minimum glucose concentration decreased by 6.2% following the application of 10% static compressive strain. Comparatively, there was a 16% decrease in the minimum glucose concentration in the degenerated IVD following compression. This decrease was more apparent in the NP region, which had a 14.7% decrease in the averaged glucose concentration following compression of the degenerated disc, as compared to a 6.8% decrease for AF region. Cell viability in normal IVD was not affected by compression. In contrast, for the degenerated IVD, the averaged cell density decreased by 3% following long-term deformation. The NP region, which had a 4% decrease in averaged cell density, was more affected than the AF, with a 2% decrease (see Fig. 5(*b*)).

Discussion

To our knowledge, this is the first study to use mechano-electrochemical mixture theory to predict nutrient distributions and cell viability in a realistic, three-dimensional IVD using finite element modeling. Our results indicate that both long-term mechanical compression and disc degeneration alter the glucose distribution in the IVD. This is because both loading and degenerative changes lead to decreased water content in the tissue. This, in turn, results in reduced pore size and a subsequent reduction in the diffusivity of solutes in the tissue. Consequently, the glucose levels in the IVD will decrease, as was seen here. For the degenerated cases, glucose levels decreased below threshold levels necessary for cell survival, and a reduction in cell density was observed.

For normal IVD, the cell density distribution did not change either with or without compression, as was expected. This is because glucose levels in the tissue did not fall below the minimum levels necessary for cell survival (i.e., 0.5 mM), see Figs. 4(*a*) and 4(*b*). This finding is in agreement with a previous study, which found no change in cell viability in the uncompressed disc with permeable cartilage endplate [33].

For the degenerated IVD, there was an 11% decrease in the cell density in the disc even without the application of compressive strain. This is in agreement with results in the literature, which indicate that cell viability was reduced in degenerated IVD and in disc having calcified endplates [33]. In general, the decrease in cell density was concentrated at the interface between the AF and NP regions of the disc (Fig. (5)), which was similar to the trend for minimum glucose concentrations (Fig. (4)). Because our criterion for cell viability was based on glucose concentrations thresholds alone, the correlation between these two factors was expected.

Our results show that nutrient levels and cell viability in the NP region are more strongly affected by the degenerative changes and deformation to the tissue, as compared to the AF region of the disc. The majority of *in vivo* (using animal model) and *in vitro* studies have suggested that the end plate route is the main pathway for exchange of solutes between the NP (and the inner AF) and the surrounding vasculature [14,16,19,20,24,62,63]. Therefore, since the reduced permeability of the endplates, used in our model to simulate endplate calcification, hinders this supply, lowered nutrient levels and subsequent cell death occurred. These findings provide important information regarding mechanisms of disc degeneration, which is found to first occur in the nucleus region of the disc [64], and the important role nutritional supply (or lack thereof) and mechanical loading play in the degeneration cascade.

Our theoretical prediction of glucose concentrations and cell density distributions in the IVD is in agreement with experimental results and theoretical analyses in the literature. For instance, our results for minimum glucose concentrations in the IVD, ranging from 0.292 to 1.748 mM, are similar to measurements in scoliotic discs reported previously [25]. Additionally, experimental studies have shown that the cell viability and nutrient levels decrease moving toward the center of the disc, further from the nutritional supply [16,20,65,66], which is in agreement with our findings particularly for the degenerated case. Likewise, results for concentration distributions of glucose in the disc are similar to those presented in previous finite element studies of the IVD (e.g., Refs. [33,36,40]).

The cell viability criteria incorporated into this model depends only on threshold levels of glucose. Previous studies have found that *p*H levels also affect cell viability, with cells beginning to die when *p*H falls below 6.8. However, it has been previously shown that the inclusion of *p*H viability criteria does not significantly affect results, when compared to those incorporating the glucose criteria alone [33]. In fact, our results indicate that the *p*H levels in the IVD did not fall below 6.8 even for the deformed, degenerated disc (data not shown). Therefore, only the glucose condition was included in the model. It should be noted, however, that results are strongly dependent upon the threshold levels chosen. In addition to glucose and *p*H levels, there are a variety of other factors that may affect cell viability and functioning, including mechanical loading, age, osmolarity, etc. Nevertheless, due to a lack of quantitative experimental data, other factors were not incorporated into the model. The levels of glucose used here were chosen based on experimental results in the literature; however, variation of these values would greatly influence the results for cell viability and glucose concentration distributions in the tissue.

As noted, our results for glucose concentration and cell density distributions in the IVD under mechanical compression represent those for the disc at equilibrium following deformation.

Therefore, these distributions are indicative of long-term compression effects on the IVD. That is, changes in cell density resulting from poor nutritional supply to cells do not occur instantaneously, but rather result from sustained nutritional shortage. Indeed, a previous study showed that cells began to die after 3 days at very low (i.e., < 0.5 mM) glucose concentrations [15]. Because of limited knowledge as to the quantitative effects of nutritional levels on cellular activity, the "real-time" consequences of such conditions have not been predicted here. Nonetheless, we believe our results give an indication of the detrimental effects of long-term deformation on the cell population in the IVD.

The model developed in this study is capable of predicting nutrient distributions, as well as stress and strain distributions, *p*H levels, osmotic pressure, etc., in the IVD. Moreover, it can be used to predict the cell density (or viability) in the IVD under a variety of conditions and therefore may serve as a powerful tool in developing new strategies for treatment and/or retardation of disc degeneration. For instance, it has been suggested that there exists an ideal window of mechanical loading in which cells can survive and function [67]. This phenomenon may be further investigated using our model, and ideal loading configurations (or exercise regimen), which allow for minimized nutrition-related cell death, may be determined; these findings may then be incorporated into a new treatment strategy for retarding or reversing disc degenerative changes.

In summary, we have developed a new theoretical model of the intervertebral disc able to predict nutrient distributions and related cell densities in the tissue. This realistic model incorporates a three-dimensional anatomical disc geometry along with strain-dependent tissue properties, nutrient transport coupled to cellular metabolism, and criteria for maintaining cell viability. Using our model, we have investigated the effects of degenerative changes and static mechanical compression on the glucose and cell density in the disc. We have found that both factors result in decreased glucose levels in the IVD. Furthermore, we have predicted a loss of cell viability in intervertebral disc with degenerative changes. These findings are a valuable supplement to experimental findings of nutrient distributions in IVD and also provide important insight into the nutrition-related mechanisms of disc degeneration, which remain to be fully delineated.

Acknowledgment

This study was supported by research grants from NIH NIAMS (Nos. AR050609 and AR056101) and NIBIB (No. EB008653) as well as an NRSA Fellowship from NIH NIA (No. AG030921).

References

[1] NIH, 1997, "Research on Low Back Pain and Common Spinal Disorders," NIH Guide 26:16.
[2] Frymoyer, J. W., and Durett, C. L., 1997, *The Adult Spine: Principles and Practice*, J. W. Frymoyer, T. B. Ducker, N. M. Hadler, J. P. Kostuik, J. N. Weinstein, and T. S. Whitecloud, eds., Lippincott-Raven, New York, pp. 143–150.
[3] Eyre, D. R., Benya, P., Buckwalter, J., Caterson, B., Heinegard, D., Oegema, T., Pearce, R., Pope, M., Urban, J., 1989, *New Perspectives on Low Back Pain*, J. W. Frymoyer and S. L. Gordon, eds., American Academy of Orthopaedic Surgeons, Park Ridge, IL, pp. 147–207.
[4] Kelsey, J. L., Mundt, D. F., and Golden, A. L., 1992, *The Lumbar Spine and Back Pain*, J. I. V. Malcolm, eds., Churchill Livingstone, New York, pp. 537–549.
[5] White, A. A., 1981, "Biomechanics of Lumbar Spine and Sacroiliac Articulation: Relevance to Idiopathic Low Back Pain," Symposium on Idiopathic Low Back Pain, A. A. White and S. L. Gordon, eds., CV Mosby Co., St. Louis, pp. 296–322.
[6] Buckwalter, J. A., 1995, "Aging and Degeneration of the Human Intervertebral Disc," Spine, **20**(11), pp. 1307–1314.
[7] Urban, J. P., Smith, S., and Fairbank, J. C., 2004, "Nutrition of the Intervertebral disc," Spine, **29**, pp. 2700–2709.
[8] Hickey, D. S., and Hukins, D. W. L., 1980, "Relation Between the Structure of the Annulus Fibrosus and the Function and Failure of the Intervertebral Disc," Spine, **5**, pp. 106–116.
[9] Marchand, F., and Ahmed, A. M., 1990, "Investigation of the Laminate Structure of Lumbar Disc Annulus Fibrosus," Spine, **15**(5), pp. 402–410.
[10] Urban, J. P., and Roberts, S., 1995, "Development and Degeneration of the Intervertebral Discs," Mol. Med. Today, **1**(7), pp. 329–335.
[11] Bibby, S. R. S., "Cell Metabolism and Viability in the Intervertebral Disc," 2002, Ph.D. dissertation, University of Oxford, Oxford, UK.
[12] Urban, J. P. G., and Roberts, S., 2003, "Degeneration of the Intervertebral Disc," Arthritis Res. Ther., **5**(3), pp. 120–130.
[13] Masuda, K., 2008, "Biological Repair of the Degenerated Intervertebral Disc by the Injection of Growth Factors," Eur. Spine J., **17**(Suppl 4), pp. S441–S451.
[14] Nachemson, A., Lewin, T., Maroudas, A., and Freeman, M. A., 1970, "In Vitro Diffusion of Dye Through the End-Plates and the Annulus Fibrosus of Human Lumbar Inter-Vertebral Discs," Acta Orthop. Scand., **41**(6), pp. 589–607.
[15] Horner, H. A., and Urban, J. P., 2001, "2001 Volvo Award Winner in Basic Science Studies: Effect of Nutrient Supply on the Viability of Cells From the Nucleus Pulposus of the Intervertebral Disc," Spine, **26**(23), pp. 2543–2549.
[16] Maroudas, A., Stockwell, R. A., Nachemson, and A., Urban, J., 1975, "Factors Involved in the Nutrition of the Human Lumbar Intervertebral Disc: Cellularity and Diffusion of Glucose In Vitro," J. Anat., **120**(1), pp. 113–130.
[17] Urban, J. P. G., Holms, S., Maroudas, A., and Nachemson, A., 1977, "Nutrition of the Intervertebral Disc: An In Vivo Study of Solute Transport," Clin. Orthop., **129**, pp. 101–114.
[18] Urban, J. P., Holm, S., and Maroudas, A., 1978, "Diffusion of Small Solutes Into the Intervertebral Disc: As In Vivo Study," Biorheology, **15**(3–4), pp. 203–221.
[19] Ogata, K., and Whiteside, L. A., 1981, "1980 Volvo Award Winner in Basic Science. Nutritional Pathways of the Intervertebral Disc. An Experimental Study Using Hydrogen Washout Technique," Spine, **6**(3), pp. 211–216.
[20] Holm, S., Maroudas, A., Urban, J. P., Selstam, G., and Nachemson, A., 1981, "Nutrition of the Intervertebral Disc: Solute Transport and Metabolism," Connect. Tissue Res., **8**(2), pp. 101–119.
[21] Crock, H. V., and Goldwasser, M., 1984, "Anatomic Studies of the Circulation in the Region of the Vertebral End-Plate in Adult Greyhound Dogs," Spine, **9**(7), pp. 702–706.
[22] Moore, R. J., Osti, O. L., Vernon-Roberts, B., and Fraser, R. D., 1992, "Changes in Endplate Vascularity After an Outer Anulus Tear in the Sheep," Spine, **17**(8), pp. 874–878.
[23] Roberts, S., Urban, J. P., Evans, H., and Eisenstein, S. M., 1996, "Transport Properties of the Human Cartilage Endplate in Relation to Its Composition and Calcification," Spine, **21**(4), pp. 415–420.
[24] Brown, M. D., and Tsaltas, T. T., 1976, "Studies on the Permeability of the Intervertebral Disc During Skeletal Maturation," Spine, **1**, pp. 240–244.
[25] Bibby, S. R., Fairbank, J. C., Urban, M. R., and Urban, J. P., 2002, "Cell Viability in Scoliotic Discs in Relation to Disc Deformity and Nutrient Levels," Spine, **27**(20), pp. 2220–2228.
[26] Ishihara, H., and Urban, J. P., 1999, "Effects of Low Oxygen Concentrations and Metabolic Inhibitors on Proteoglycan and Protein Synthesis Rates in the Intervertebral Disc," J. Orthop. Res., **17**(6), pp. 829–835.
[27] Ohshima, H., and Urban, J. P., 1992, "The Effect of Lactate and *p*H on Proteoglycan and Protein Synthesis Rates in the Intervertebral Disc," Spine, **17**(9), pp. 1079–1082.
[28] Grunhagen, T., Wilde, G., Soukane, D. M., Shirazi-Adl, S. A., and Urban, J. P. G., 2006, "Nutrient Supply and Intervertebral Disc Metabolism," J. Bone Joint Surg. Am., **88**, pp. 30–35.
[29] Risbud, M. V., Guttapalli, A., Stokes, D. G., Hawkins, D., Danielson, K. G., Schaer, T. P., Albert, T. J., and Shapiro, I. M., 2006, "Nucleus Pulposus Cells Express HIF-1alpha Under Normoxic Culture Conditions: A Metabolic Adaptation to the Intervertebral Disc Microenvironment," J. Cell. Biochem., **98**, pp. 152–159.
[30] Lee, D. C., Adams, C. S., Albert, T. J., Shapiro, I. M., Evans, S. M., and Koch, C. J., 2007, "In Situ Oxygen Utilization in the Rat Intervertebral Disc," J. Anat., **210**, pp. 294–303.
[31] Johnson, W. E. B., Stephan, S., and Roberts, S., 2008, "The Influence of Serum, Glucose and Oxygen on Intervertebral Disc Cell Growth In Vitro: Implications for Degenerative Disc Disease," Arthritis Res. Ther., **10**(2), pp. R46.
[32] Bibby, S. R., and Urban, J. P., 2004, "Effect of Nutrient Deprivation on the Viability of Intervertebral Disc Cells," Eur. Spine J., **13**(8), pp. 695–701.
[33] Shirazi-Adl, A., Taheri, M., and Urban, J. P., 2010, "Analysis of Cell Viability in Intervertebral Disc: Effect of Endplate Permeability on Cell Population," J. Biomech., **43**(7), pp. 1330–1336.
[34] Guehring, T., Wilde, G., Sumner, M., Grünhagen, T., Karney, G. B., Tirlapur, U. K., and Urban, J. P., 2009, "Notochordal Intervertebral Disc Cells: Sensitivity to Nutrient Deprivation," Arthritis Rheum., **60**(4), pp. 1026–1034.
[35] Huang, C.-Y., and Gu, W. Y., 2008, "Effects of Mechanical Compression on Metabolism and Distribution of Oxygen and Lactate in Intervertebral Disc," J. Biomech., **41**(6), pp. 1184–1196.
[36] Soukane, D. M., Shirazi-Adl, A., and Urban, J. P. G., 2009, "Investigation of Solute Concentrations in a 3D Model of Intervertebral Disc," Eur. Spine J., **18**, pp. 254–262.
[37] Soukane, D. M., Shirazi-Adl, A., and Urban, J., 2005, "Analysis of Nonlinear Coupled Diffusion of Oxygen and Lactic Acid in Intervertebral Discs," J. Biomech. Eng., **127**(7), pp. 1121–1126.
[38] Soukane, D. M., Shirazi-Adl, A., and Urban, J. P., 2007, "Computation of Coupled Diffusion of Oxygen, Glucose and Lactic Acid in an Intervertebral Disc," J. Biomech., **40**(12), pp. 2645–2654.
[39] Selard, E., Shirazi-Adl, A., and Urban, J., 2003, "Finite Element Study of Nutrient Diffusion in the Human Intervertebral Disc," Spine, **28**(17), pp. 1945–1953.
[40] Magnier, C., Boiron, O., Wendling-Mansuy, S., Chabrand, P., and Deplano, V., 2009, "Nutrient Distribution and Metabolism in the Intervertebral Disc

in the Unloaded State: A Parametric Study," J. Biomech., **42**(2), pp. 100–108.
[41] Jackson, A. R., Huang, C.-Y., and Gu, W. Y., 2011, "Effect of Endplate Calcification and Mechanical Deformation on the Distribution of Glucose in Intervertebral Disc: A 3D Finite Element Study," Comp. Meth. Biomech. Biomed. Eng., **14**(2), pp. 195–204.
[42] Lai, W. M., Hou, J. S., and Mow, V. C., 1991, "A Triphasic Theory for the Swelling and Deformation Behaviors of Articular Cartilage," J. Biomech. Eng., **113**(3), pp. 245–258.
[43] Gu, W. Y., Yao, H., Huang, C.-Y., and Cheung, H. S., 2003, "New Insight Into Deformation-Dependent Hydraulic Permeability of Gels and Cartilage, and Dynamic Behavior of Agarose Gels in Confined Compression," J. Biomech., **36**, pp. 593–598.
[44] Gu, W. Y., Yao, H., Vega, A. L., and Flagler, D., 2004, "Diffusivity of Ions in Agarose Gels and Intervertebral Disc: Effect of Porosity," Ann. Biomed. Eng., **32**, pp. 1710–1717.
[45] Thompson, J. P., Pearce, R. H., Schechter, M. T., Adams, M. E., Tsang, I. K. Y., and Bishop, P. B., 1990, "Preliminary Evaluation of a Scheme for Grading the Gross Morphology of the Human Intervertebral Disc," Spine, **15**, pp. 411–415.
[46] Sun, D. N., Gu, W. Y., Guo, X. E., Lai, W. M., and Mow, V. C., 1999, "A Mixed Finite Element Formulation of Triphasic Mechano-Electrochemical Theory for Charged, Hydrated Biological Soft Tissues," Int. J. Numer. Methods Eng., **45**, pp. 1375–1402.
[47] Yao, H., and Gu, W. Y., 2004, "Physical Signals and Solute Transport in Cartilage Under Dynamic Unconfined Compression: Finite Element Analysis," Ann. Biomed. Eng., **32**, pp. 380–390.
[48] Yao, H., and Gu, W. Y., 2007, "Three-Dimensional Inhomogeneous Triphasic Finite-Element Analysis of Physical Signals and Solute Transport in Human Intervertebral Disc Under Axial Compression," J. Biomech., **40**(9), pp. 2071–2077.
[49] Roberts, S., Menage J., Urban, J. P., 1989, "Biochemical and Structural Properties of the Cartilage End-Plate and Its Relation to the Intervertebral Disc," Spine, **14**(2), pp. 166–174.
[50] Setton, L. A., Zhu, W., Weidenbaum, M., Ratcliffe, A., and Mow, V. C., 1993, "Compressive Properties of the Cartilaginous End-Plate of the Baboon Lumbar Spine," J. Orthop. Res., **11**(2), pp. 228–239.
[51] Gu, W. Y., and Yao, H., 2003, "Effects of Hydration and Fixed Charge Density on Fluid Transport in Charged Hydrated Soft Tissue," Ann. Biomed. Eng., **31**(10), pp. 1162–1170.
[52] Maroudas, A., 1975, "Biophysical Chemistry of Cartilaginous Tissues With Special Reference to Solute and Fluid Transport," Biorheology, **12**, pp. 233–248.
[53] Iatridis, J. C., Kumar, S., Foster, R. J., Weidenbaum, M., and Mow, V. C., 1999, "Shear Mechanical Properties of Human Lumbar Annulus Fibrosus," J. Orthop. Res., **17**(5), pp. 732–737.
[54] Iatridis, J. C., Setton, L. A., Weidenbaum, M., and Mow, V. C., 1997, "Alterations in the Mechanical Behavior of the Human Lumbar Nucleus Pulposus With Degeneration and Aging," J. Orthop. Res., **15**(2), pp. 318–322.
[55] Johannessen, W., and Elliot, D. M., 2005, "Effects of Degeneration on the Biphasic Material Properties of Human Nucleus Pulposus in Confined Compression," Spine, **30**(24), pp. E724–E729.
[56] Bernick, S., and Cailliet, R., 1982, "Vertebral End-Plate Changes With Aging of Human Vertebrae," Spine, **7**(2), pp. 97–102.
[57] Roberts, S., Menage, J., and Eisenstein, S. M., 1993, "The Cartilage End-Plate and Intervertebral Disc in Scoliosis: Calcification and Other Sequelae," J. Orthop. Res., **11**(5), pp. 747–757.
[58] Urban, M. R., Fairbank, J. C., Etherington, P. J., Loh, F. L., Winlove, C. P., and Urban, J. P., 2001, "Electrochemical Measurement of Transport Into Scoliotic Intervertebral Discs In Vivo Using Nitrous Oxide as a Tracer," Spine, **26**(8), pp. 984–990.
[59] Nguyen-Minh, C., Haughton, V. M., Papke, R. A., An, H., Censky, and S. C., 1998, "Measuring Diffusion of Solutes Into Intervertebral Disks With MR Imaging and Paramagnetic Contrast Medium," AJNR Am. J. Neuroradiol., **19**(9), pp. 1781–1784.
[60] Huang, C.-Y., Yuan, T.-Y., Jackson, A. R., Hazbun, L., and Gu, W. Y., 2007, "Effects of Low Glucose Concentrations on Oxygen Consumption Rates of Intervertebral Disc Cells," Spine, **32**(19), pp. 2063–2069.
[61] Bibby, S. R. S., Jones, D. A., Ripley, R. M., and Urban, J. P., 2005, "Metabolism of the Intervertebral Disc: Effects of Low Levels of Oxygen, Glucose, and pH on Rates of Energy Metabolism of Bovine Nucleus Pulposus Cells," Spine, **30**(5), pp. 487–496.
[62] Brodin, H., 1955, "Path of Nutrition in Articular Cartilage and Intervertebral Disk," Acta Ortho. Scand., **24**, pp. 177.
[63] Urban, J. P., Holm, S., Maroudas, A., and Nachemson, A., 1982, "Nutrition of the Intervertebral Disc: Effect of Fluid Flow on Solute Transport," Clin. Orthop., **170**, pp. 296–302.
[64] Haefeli, M., Kalberer, F., Saegesser, D., Nerlich, A. G., Boos, N., and Paesold, G., 2006, "The Course of Macroscopic Degeneration in the Human Lumbar Intervertebral Disc," Spine, **31**(14), pp. 1522–1531.
[65] Urban, M. R., Fairbank, J. C., Bibby, S. R., and Urban, J. P., 2001, "Intervertebral Disc Composition in Neuromuscular Scoliosis: Changes in Cell Density and Glycosaminoglycan Concentration at the Curve Apex," Spine, **26**(6), pp. 610–617.
[66] Bartels, E. M., Fairbank, J. C., Winlove, C. P., and Urban, J. P., 1998, "Oxygen and Lactate Concentrations Measured In Vivo in the Intervertebral Discs of Patients With Scoliosis and Back Pain," Spine, **23**(1), pp. 1–7.
[67] Stokes, I. A., and Iatridis, J. C., 2004, "Mechanical conditions that accelerate intervertebral disc degeneration: overload versus immobilization," Spine, **29**(23), pp. 2724-2732.